

# RSC Advances



This is an *Accepted Manuscript*, which has been through the Royal Society of Chemistry peer review process and has been accepted for publication.

*Accepted Manuscripts* are published online shortly after acceptance, before technical editing, formatting and proof reading. Using this free service, authors can make their results available to the community, in citable form, before we publish the edited article. This *Accepted Manuscript* will be replaced by the edited, formatted and paginated article as soon as this is available.

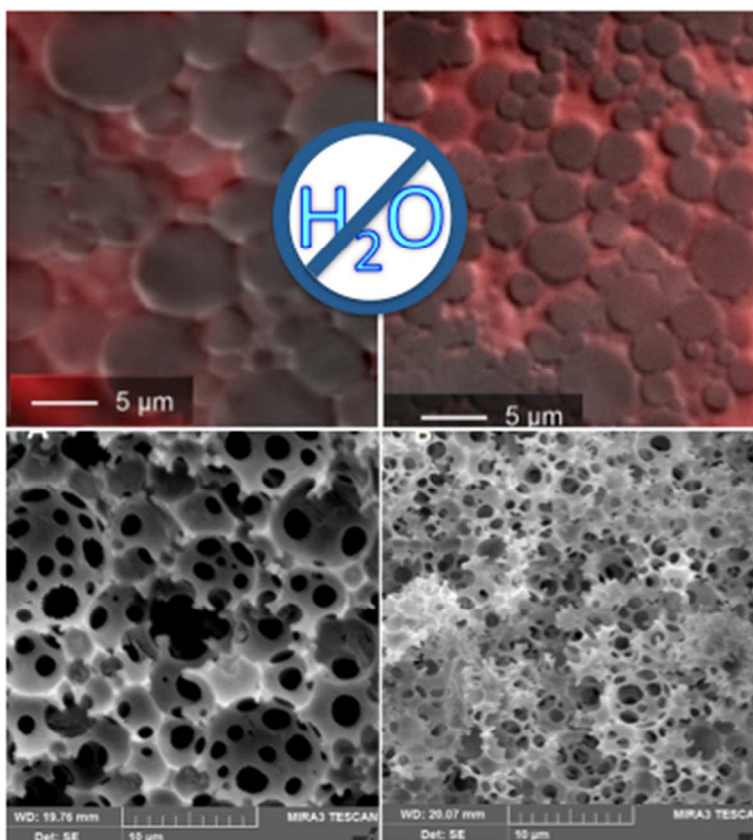
You can find more information about *Accepted Manuscripts* in the [Information for Authors](#).

Please note that technical editing may introduce minor changes to the text and/or graphics, which may alter content. The journal's standard [Terms & Conditions](#) and the [Ethical guidelines](#) still apply. In no event shall the Royal Society of Chemistry be held responsible for any errors or omissions in this *Accepted Manuscript* or any consequences arising from the use of any information it contains.

## Table of Contents

**Porous monoliths synthesized via polymerization of styrene and divinyl benzene in nonaqueous deep-eutectic solvent-based HIPEs**

M. G. Pérez-García, A. Carranza, J. E. Puig, J. A. Pojman, F. del Monte,\* G. Luna-Bárcenas,\* and J. D. Mota-Morales\*



Due to their viscosity and polarity, DESs represent a suitable internal phase for HIPEs containing styrenic monomers in addition to acrylates, thus expanding on the range of monomers forming polymerizable DES-based HIPEs.

## ARTICLE

## Porous monoliths synthesized via polymerization of styrene and divinyl benzene in nonaqueous deep-eutectic solvent-based HIPEs

Cite this: DOI: 10.1039/x0xx00000x

M. G. Pérez-García,<sup>a,d</sup> A. Carranza,<sup>b</sup> J. E. Puig,<sup>c</sup> J. A. Pojman,<sup>b</sup> F. del Monte,<sup>\*a</sup> G. Luna-Bárcenas,<sup>\*d</sup> and J. D. Mota-Morales<sup>\*e</sup>

Received 00th January 2012,  
Accepted 00th January 2012

DOI: 10.1039/x0xx00000x

www.rsc.org/

Stable nonaqueous high internal phase emulsions (HIPEs) were prepared and thermally polymerized to yield poly(HIPEs). The internal phase accounting for 80 vol.% of the HIPE consisted of a deep-eutectic solvent (DES) while the continuous one comprised styrene and divinyl benzene in a 10:1 molar ratio. DESs with different viscosities were used as an internal phase: choline chloride combined with urea, glycerol or ethylene glycol in a 1:2, salt:hydrogen bond donor molar ratio, respectively. HIPEs were stabilized with different amounts of the surfactant Span 60 (10, 20 and 50 wt.% with respect to the total amount of monomers). DESs viscosity and the amount of surfactant employed impact the morphology and mechanical properties of poly(HIPEs). Resulting poly(HIPEs) showed interconnected porosity and high thermal stability above 310°C. It's worth noting that DES was recovered from 89 to nearly 95 wt.% and the monomer conversion was as high as 0.96. In addition, water-in-oil HIPEs were stabilized and then polymerized under the same conditions, but the porous structure of the resulting poly(HIPEs) collapsed. This research demonstrates that DESs are a suitable internal phase for HIPEs thus expanding on the range of monomers forming polymerizable DES-based HIPEs.

### Introduction

High internal phase emulsions (HIPEs) are characterized by an internal phase volume fraction exceeding 0.74, which is the critical value of the most compact arrangement of uniform spherical droplets in a given volume.<sup>1-3</sup> HIPEs structure generally consists of polyhedral and polydisperse droplets separated by a thin film of continuous phase.<sup>4</sup> HIPEs have been used in a variety of industries including food and cosmetics.

One of the most interesting application of HIPEs is their use as templates to obtain porous polymeric materials, commonly called poly(HIPEs).<sup>5</sup> The process consists of polymerizing the continuous phase surrounding the internal phase droplets, followed by solidification of the continuous phase, which results in the embedding of the emulsion droplets in the final material. Subsequent removal of the internal phase yields a porous replica of the emulsion.<sup>6</sup> Poly(HIPEs) have been prepared for a diverse range of applications including supports for solid phase synthesis,<sup>7</sup> adsorbents,<sup>8,9</sup> electrochemical sensors,<sup>10</sup> tissue engineering scaffolds<sup>11</sup> and controlled drug delivery<sup>12</sup> among others.

From the synthetic viewpoint, poly(HIPEs) are attractive porous materials because their morphologies and mechanical properties can be modified by varying surfactant composition, concentration of the external phase and polymerization conditions.<sup>5,13,14</sup> The most common routes for poly(HIPEs) synthesis involve water or aqueous solutions as internal phases. Despite the wide range of morphologies available through wet approaches, the polymerization mechanisms and conditions

have been limited by the presence of water due to sensitivity to moisture or evaporation. Though sporadically, nonaqueous systems have also been reported. For instance, ordered porous ceramics using oil-in-formamide emulsions<sup>15</sup> as well as self-assembly of colloidal systems in ethanol.<sup>16</sup> Cameron and Sherrington<sup>17</sup> demonstrated the synthesis of nonaqueous poly(HIPEs) using N,N'-dimethyl acetamide and dimethyl sulfoxide as internal phase. Hariri et al.<sup>18</sup> devised an oil-in-oil HIPE where both phases can polymerize, and recently Cai et al.<sup>19</sup> reported a Pickering oil-in-oil HIPE stabilized by chemically modified fumed silica.

Within the frame of green chemistry, ionic liquids<sup>20-23</sup> and supercritical fluids<sup>24-27</sup> have been used as internal phase for poly(HIPE) synthesis. Ionic liquids are aimed to develop new nonaqueous routes for poly(HIPE) synthesis; besides, they can be reused, bringing sustainability to the processes. In a recent approach, Carranza et al.<sup>28</sup> demonstrated that deep-eutectic solvents (DES) are an attractive alternative for the sustainable nonaqueous synthesis of porous polyacrylates. Methacrylate and acrylate-based HIPEs were polymerized under normal and low pressure thanks to the negligible volatility of DES, thus significantly expanding on the polymerization conditions available for poly(HIPE)s synthesis. In that work up to 95 % of the DES was recovered and the conversion of monomer was as high as 99 %.

DESs are a type of ionic liquids comprised of a eutectic mixture of hydrogen bond donor (HBD) and ammonium or phosphonium salts.<sup>29</sup> DESs are a new generation of green solvents that have received a great deal of attention due to their

low cost, biocompatibility, negligible vapor pressure, high thermal and chemical stabilities, their ability to dissolve both ionic and organic solutes, and the easiness to prepare them with high purity.<sup>30-32</sup> Through an enhanced polymerization of HIPEs in a nonaqueous environment and internal phase's reusability, DESs can provide an alternative green tool in the creation of hierarchically porous materials in a sustainable manner.

In this work, the use of DESs with different viscosities (choline chloride combined with urea, glycerol or ethylene glycol) as an alternative internal phase for the nonaqueous synthesis of styrenic poly(HIPEs) is proposed. The effect of both DESs' viscosities and amount of surfactant employed, on the porous structure and mechanical properties of poly(HIPEs) is systematically studied. The mechanical and structural properties of polymerized DES-in-oil HIPEs are compared with water-in-oil HIPEs polymerized under identical conditions. Finally, due to their viscosity and polarity, DESs represent a suitable internal phase for HIPEs containing styrenic monomers in addition to acrylates, thus expanding on the range of monomers forming polymerizable DES-based HIPEs.

## Experimental

Styrene (St) and divinyl benzene (DVB), 99 % pure from Sigma Aldrich, were passed through DH-4 column (Scientific Polymeric Products) to remove the inhibitor (4-tert-butylcatechol). 2,2'-Azobis(2-methylpropionitrile) (AIBN) 97 % pure from Sigma Aldrich was recrystallized from methanol. Urea (U) 99 % pure, choline chloride (ChCl) 98 % pure, glycerol (G) 99 % pure and ethylene glycol (EG) anhydrous 99.8 % pure were purchased from Sigma Aldrich. The surfactant Span 60, (sorbitan stearate with a hydrophilic-lipophilic balance, HLB = 4.7) was from Sigma Aldrich. Doubly distilled and deionized water was employed.

HIPEs were prepared by the conventional method, which consists of stepwise addition with stirring of the disperse phase (DES or water) to the continuous phase (mixture of monomers, surfactant and initiator) at 25 °C. Agitation at 300 rpm was applied with a vibromixer. The continuous phase (20 vol.%) consisted in St and DVB in a 10:1 molar ratio, 1 wt.% AIBN (with respect to the total amount of monomers) and surfactant. The amount of surfactant used was 50, 20 or 10 wt.% with respect to the total amount of monomers. To prepare the internal nonaqueous DES phase (80 vol.%), ChCl was combined with U, G or EG in a 1:2 molar ratio. The mixture was heated at 60 °C until a clear viscous, homogeneous liquid was obtained. ChCl was oven dried at 90 °C before used. The obtained HIPEs with the different internal phases were polymerized in an oven at 60 °C for 24 h. After polymerization, the internal phase and the surfactant were removed by a Soxhlet solvent extraction, and by washing with methanol for 12 h. Finally, the monoliths were dried at room temperature until constant weight was reached. All poly(HIPEs) were labelled according to the first letter of the HBD used (or in the case of water with the letter "W") and the amount of surfactant.

Conversion was determined by dividing the mass of the dried monolith by its expected mass. The methanol washes (containing the DESs dissolved components) were dried until constant weight. The percentage of recovered DES was calculated by dividing the mass of recovered DES by its expected recovered mass. The poly(HIPEs') bulk density was estimated by measuring the volume of monoliths with regular shape.

HIPEs were observed using deconvolution fluorescent microscopy (Leica DM RXA2). The monomers phase was

marked with the fluorescent dye rhodamine B (Sigma Aldrich) as a fluorescent marker to discern the place of each component. The average droplet size was determined using ImageJ analysis software.

The macroporous structure of the monoliths was observed by field emission scanning electron microscopy (FESEM, Mira from TESCAN) with accelerating voltage of 15kV. All samples were gold-coated for 120 s in an argon atmosphere (Emitech 550). The average pore and pore window diameters were calculated in sets of 100 using ImageJ Analysis Software. Nitrogen adsorption/desorption isotherms were determined at 77 K with a Quantachrome Instruments Autosorb IQ. The specific surface area was calculated by the Brunauer-Emmett-Teller (BET) equation from the adsorption isotherm over a relatively low-pressure range (0.1–0.3 P/P<sub>0</sub>).

The poly(HIPEs) thermal stability was assessed by thermogravimetric analysis (TA Discovery thermogravimetric analyzer) in an inert nitrogen atmosphere from 20 to 700 °C with a heating rate of 10 °C min<sup>-1</sup>. Thermal analysis was performed using the TA Universal Analysis Software.

Compression tests on the monoliths were carried out according to the standard ASTM D 1621 method in an Instron 4411 with a 5KN load cell and a platen speed of 1 in min<sup>-1</sup>. The samples were compressed to 75 % of their initial height. Elastic modulus was determined from the initial linear slope of the stress-strain curve. In addition, the stress at yield was recorded to give the crush or compression strength.

## Results and Discussion

Choline chloride (ChCl) salt was combined with U, G or EG in a 1:2 molar ratio to obtain DESs with different viscosities: 750,<sup>33</sup> 250 and 37 cP (at 25 °C), respectively.<sup>34</sup> DESs or water were used as the internal phase for the formation of HIPEs. The continuous phase consisted of St and DVB in 10:1 molar ratio; in this way the homogeneity of the physical properties of resulting poly(HIPEs) is maintained because of the similarity in chemical structures of St and DVB. Researchers at Unilever<sup>35</sup> discovered that the surfactant used to form w/o HIPEs must have a low hydrophilic/lipophilic balance (HLB) value, between 2 and 6. The surfactant employed here was sorbitan monooleate (commonly known as Span 60), which has an HLB of 4.7. The amount of surfactant was 10, 20 or 50 wt.% with respect to the total amount of monomers. The resulting HIPEs with the different internal phases were stable, had a white aspect and presented high viscosity such that they did not flow upon inversion of their containers (Fig. 1).

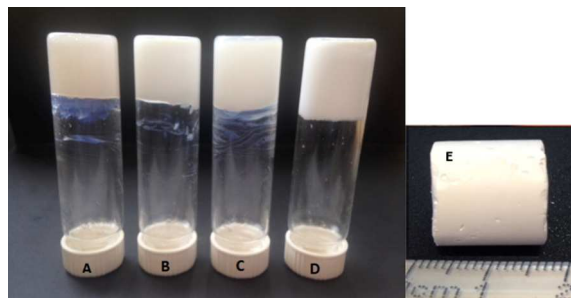


**Figure 1.** Images of HIPEs with different internal phases: A) HIPE-U20, B) HIPE-G20, C) HIPE-E20 and D) HIPE-W20, E) Final monolith after DES extraction.



**Table 1.** Stability of HIPEs and poly(HIPEs) by visual observation, conversion based on gravimetry of poly(HIPEs), percentage of recovered DES after wash, and compression analysis of poly(HIPEs).

HIPE	Stability (25 °C)	Poly (HIPE) Stability	Conv. [%]	DES recovered	Compression analysis [psi]	
					Elastic modulus	Crush strength
HIPE-U10	< 3 days	good	96	91	3685	218
HIPE-U20	< 3 days	good	94	89	1057	126
HIPE-U50	< 3 days	crumbled	-	-	-	-
HIPE-G10	ps	-	-	-	-	-
HIPE-G20	< 1 day	good	93	91	3129	270
HIPE-G50	< 1 day	crumbled	-	-	-	-
HIPE-E10	ps	-	-	-	-	-
HIPE-E20	< 5 hours	fragile	91	95	211	18
HIPE-E50	< 5 hours	crumbled	-	-	-	-
HIPE-W10	< 1 day	fragile	91	-	nd	nd
HIPE-W20	< 1 day	fragile	95	-	131	22
HIPE-W50	< 1 day	crumbled	-	-	-	-

ps: phase separation. nd: not determined. Conv.: Conversion.

Emulsion stability was affected by the type of internal phase and the amount of surfactant used; results are reported in Table 1. The high viscosity of the internal phase reduces drastically the Ostwald ripening effect, thus preventing the continuous phase's thin walls from collapsing and the HIPEs from breaking.<sup>36</sup> It was reported that solvatophobic interactions between ionic liquid counterions and the hydrocarbon portion of surfactants,<sup>37</sup> as well as the cation-anion interaction,<sup>38</sup> greatly modify the cloud point of nonionic surfactants. The significant influence on the behavior of solute molecules by ionic liquids can be taken as an extreme case of the effect of adding salt to the disperse phase of water-in-oil emulsions,<sup>39</sup> which dramatically stabilize emulsions through a decreased of the surfactant's cloud point. Taking this into account, Carranza et al.<sup>28</sup> proposed that DESs have an effect similar to adding a salt to a HIPE's internal phase and analogue to the effect of ionic liquids.

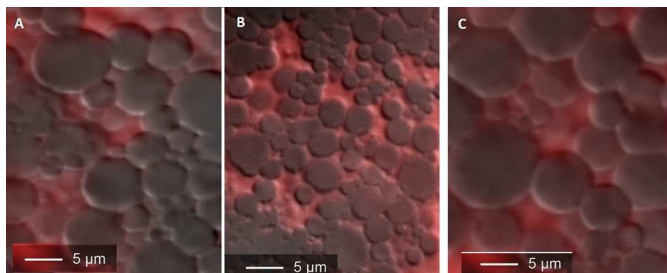


**Figure 2.** Deconvolution fluorescent micrographs of HIPEs A) HIPE-U10, B) HIPE-U20 and C) HIPE-G20.

These researchers suggested that DESs enhance the HIPEs stability through a decrease of the surfactant's cloud point, besides to a relatively high viscosity provided by the proper balance between the component's polarities. In this work it is demonstrated that DESs having higher viscosity showed better

stability at both room temperature and 60 °C, further supporting the hypothesis that viscosity of DES (as continuous phase) helps stabilizing HIPEs (Table 1).

Deconvolution fluorescent microscopy images of HIPE-U10, HIPE-U20 and HIPE-G20 are shown in Fig. 2. The structure consisted of close packed polyhedral and polydisperse droplets separated by a thin film of continuous phase, which is characteristic of HIPEs. To identify each phase in the emulsions, the monomer/crosslinker continuous phase was marked by the fluorescent dye rhodamine B. Fluorescent images of HIPEs-E and HIPEs-W were not acquired due to the low stability of the emulsions (droplets collapsed during observation).

HIPEs were polymerized thermally with AIBN at 60 °C to yield poly(HIPEs). Poly(HIPEs') stability was determined by visually and values are reported in Table 1. As expected, poly(HIPEs) that presented good stability maintained the shape and volume of the vessel where the precursor emulsions were prepared (Fig. 1E). Table 1 also reports conversion of the monoliths synthesized and DES recovered. The wash containing DES components was freeze-dried and weighed. DES was recovered from 89 to nearly 95 wt.%. Dried monolith conversion was determined gravimetrically.

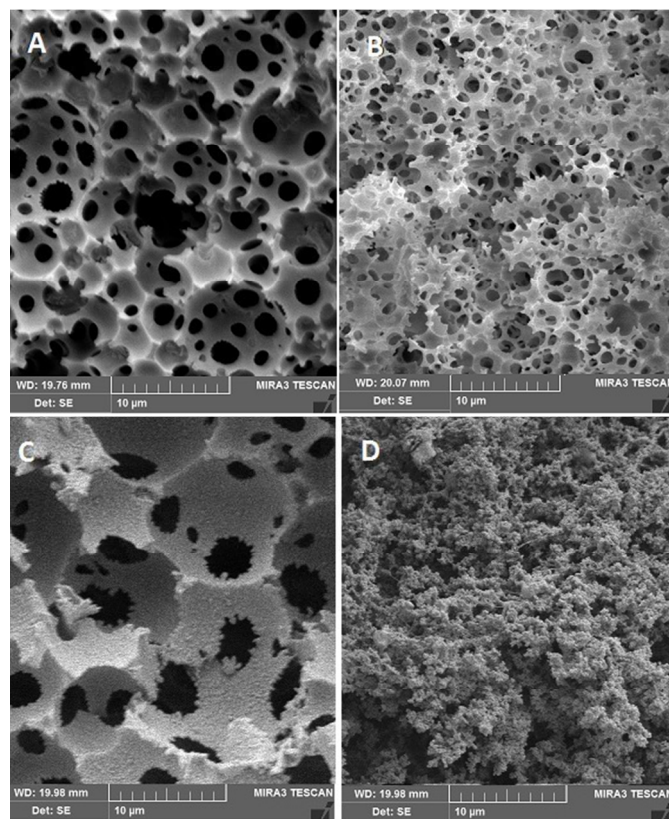


**Figure 3.** FESEM micrographs of poly(HIPEs) after DES or water extraction: A) Poly(HIPE)-U10, B) Poly(HIPE)-U20, C) Poly(HIPE)-G20 and D) Image represents structure of poly(HIPEs)-W10, W20 and E20.

All poly(HIPEs) had high conversions between 91 and 96 wt.%. These results were similar to the ones obtained by Carranza et al.<sup>28</sup> for different methacrylates and acrylates HIPEs with U:ChCl as internal phase. Interestingly, conversion was not affected by the type of internal phase because polymerization takes place in the phase around the droplets of

internal phase which acts as templates to obtain the porous structure.

The structure of all the monoliths (listed in Table 1) was observed by field emission electron microscopy (FESEM). FESEM images of poly(HIPE)-U10 (Fig. 3a), poly(HIPE)-U20 (Fig. 3b) and poly(HIPE)-G20 (Fig. 3c) show that poly(HIPEs) macroporous structure consists of a pore network with cells interconnected through narrow necks (or pore windows). The pore size was similar to the droplet size of the HIPE used as template, as shown in Table 2.

**Table 2.** Structural morphology of HIPEs and poly(HIPEs)

HIPE	$S_{\text{BET}}$ [m <sup>2</sup> g <sup>-1</sup> ]	Con- focal [μm]	FE- SEM [μm]	Pore window [μm]	Degree of openness [%]	$\rho_b$ [g cm <sup>-3</sup> ]	$V_T$ [cm <sup>3</sup> g <sup>-1</sup> ]
Poly (HIPE)- U10	4.2	5±1.8	5±1.3	1.2±0.44	11.7	0.21	3.8
Poly (HIPE)- U20	6.9	2±0.7	3±0.8	0.87±0.2	28.5	0.17	5
Poly (HIPE)- G20	2.6	7±1.7	8±3.2	2.07±1.3	9.2	0.23	3.4

$S_{\text{BET}}$ : Specific Surface Area.  $\rho_b$ : Bulk density monolith.  $V_T$ : total pore volume

Droplet size did not change significantly during polymerization and the structure of these monoliths is an approximate replica of the emulsion. It is worth mentioning that droplet size of the HIPEs (or pore size of the poly(HIPE)) decreases as the amount of surfactant increased; the same occurs with DES viscosity (Fig. 4). An increase in the droplet size of the emulsions can be attributed to coalescence between droplets, which means that larger droplets grow at the expense of smaller ones.<sup>40,41</sup> The amount of coalescence was found to decrease with increasing surfactant amount which explains the results obtained here (Fig. 4). In addition, high viscosity of the internal phase also prevents coalescence,<sup>36</sup> hence the droplet size of HIPE-U20 is smaller than the one of HIPE-G20 using the same amount of surfactant (Table 2). The porous structure of poly(HIPEs)-E20, W10, W20 and W50 collapsed (Fig. 3d) due to the low stability of HIPEs during polymerization at 60 °C. In a previous work<sup>41</sup> surfactants with higher molecular weight or a salt dissolved in the internal phase were used to enhance stability of styrene/divinylbenzene/surfactant/water HIPEs.

Pore and pore window diameters calculated in sets of 100 through image analysis were used to estimate poly(HIPEs) degree of openness with the equation proposed by Pulko and Krajnc<sup>42</sup> (Scheme S1). Pore window diameter differed from poly(HIPE)-U10 to poly(HIPE)-U20 resulting in unique degree of openness attributed to the amount of surfactant employed. The degree of openness of poly(HIPE)-U20 was higher than the one of poly(HIPE)-U10 because at slightly higher surfactant amount, the layer of oil between DES droplets thins and begins to retract at points where DES droplets touch each other. This leads to a bigger opening in the cell wall.<sup>43</sup> As the surfactant amount increased, the thin oil layer retracts even more until it disappears. Poly(HIPEs)-U50 and G50 crumbled because the amount of surfactant was too high and the monoliths generated under these conditions have no walls, only struts, similarly to water/surfactant/styrene system reported.<sup>40</sup>

The above results show the dramatic influence of the surfactant-to-monomer ratio and the internal phase viscosity on the monolith microstructure. On the other hand, monolith microstructure plays an important role on the mechanical

properties, which are a measure of the general usefulness of a given material. Compression analyses of poly(HIPEs)-U10, U20, G20, E20 and W20 were made to evaluate the influence of the different porous structure obtained on both the elastic modulus and crush strength. Stress-strain curves (Fig. S1) were similar to the ones obtained for reduced density materials and low-density foams<sup>40, 44</sup> Elastic modulus was determined from the initial linear slope of the stress-strain curve and the stress at yield was recorded to give the crush or compression strength; results are reported in Table 1. Poly(HIPEs)-U10, U20 and G20 have the highest values of elastic modulus and crush strength. As expected, poly(HIPEs)-E20 and W20 have the lowest values because the porous structure collapsed.

The bulk density ( $\rho_b$ ) of poly(HIPEs)-U10, U20 and G20 estimated by measuring the volume of monoliths with regular shape was used to obtain the total pore volume ( $V_T$ ), calculated from  $1/\rho_b - 1/\rho_w$ , where  $\rho_w$  is the wall density, which was assumed to be the polymer density (1.05 g mL<sup>-1</sup>). These values of  $\rho_b$  and  $V_T$  (Table 2) are similar to other macroporous materials reported in the literature.<sup>35,45</sup> Moreover, it is evident that the  $V_T$  has an important influence on compressive properties, since elastic modulus and crush strength increase as  $V_T$  decreases, as is reported in Tables 1 and 2.

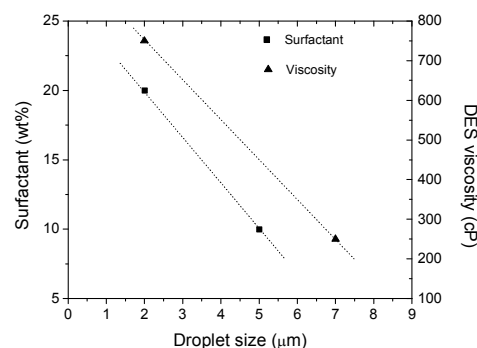


**Figure 4.** Effect of amount of surfactant and DES viscosity on droplet size of HIPEs. (Viscosity values were taken from Zhang et al.<sup>34</sup>)

Information about the porosity of poly(HIPEs)-U10, U20 and G20 was obtained by nitrogen adsorption/desorption isotherms (Fig. S3). The purified monoliths showed an isotherm with narrow hysteresis loop and small adsorption at low pressure, which indicates the absence of micropores and mesopores. The BET analysis showed small surface area values of a few m<sup>2</sup> g<sup>-1</sup> for all the monoliths analyzed where poly(HIPE)-U20 had the highest surface area of 6.9 m<sup>2</sup> g<sup>-1</sup> (Table 2). Although the morphology of the materials is highly porous and interconnected, the relative large pore size results in a low surface area, which is typical for macroporous materials.<sup>20,22,23,28,46,47</sup> Finally, the thermogravimetric analysis (TGA) revealed that all poly(HIPEs) presented high thermal stability above 310 °C (Fig. S2, Table S1).

## Conclusions

In this work we demonstrated that DESs represent a suitable internal phase for HIPEs containing styrenic monomers in addition to acrylates and methacrylates, thus expanding on the range of monomers with different polarity and chemical structure forming polymerizable DES-based HIPEs. Furthermore, we proposed the use of DESs with different viscosities as internal phase to obtain stable nonaqueous HIPEs.

Stability and morphology of HIPEs was affected by the amount of surfactant and viscosity of different DESs. Stable HIPEs were thermally polymerized to obtain interconnected styrenic macroporous materials, which presented high thermal stability above 310 °C. DES was recovered from 89 to ca. 95 wt.% and the conversion of monomer was as high as 96 wt.%. Moreover, we have also demonstrated that porous structure had an important influence on mechanical properties of poly(HIPEs). Porous structure can be easily modified by varying both, the amount of surfactant or DES's viscosity. This work supports that DESs provide an attractive alternative mean for the sustainable nonaqueous synthesis of porous materials consisting in a wide range of monomers' chemistry and polarity.

## Acknowledgements

The authors gratefully acknowledge Dr. Ruben Gonzalez Nuñez for the use of his compression tests instrument, Dr. Sergio Gomez Salazar for BET analysis and Dr. Israel Ceja Andrade for his assistance in the FESEM observations. This paper was written under the auspices of CONACYT through *Estancias postdoctorales en el extranjero* and *Cátedras CONACYT* programs, for which MGPG and JDMM are grateful. GLB acknowledges CONACYT project 181678.

## Notes and references

<sup>a</sup> Instituto de Ciencia de Materiales de Madrid-ICMM, Consejo Superior de Investigaciones Científicas-CSIC Campus Cantoblanco, 28049 Madrid, Spain.

E-mail: delmonte@icmm.csic.es

<sup>b</sup> Department of Chemistry, Louisiana State University, Baton Rouge, Louisiana 70803, USA.

<sup>c</sup> Ingeniería Química, Universidad de Guadalajara, Guadalajara, Jalisco 44430, Mexico.

<sup>d</sup> Centro de Investigación y de Estudios Avanzados Unidad Querétaro, Querétaro 76230 México.

E mail: gluna@qro.cinvestav.mx

<sup>e</sup> Cátedras Conacyt al Centro de Nanociencias y Nanotecnología-UNAM, Ensenada, Baja California 22860 México.

E-mail: mota\_josue@hotmail.com; jmota@cnyun.unam.mx

Electronic Supplementary Information (ESI) available: details of compression analysis, TGA, porosimetry analysis and calculation of the degree of openness. See DOI: 10.1039/b000000x/

1. K. J. Lissant, *Journal of Colloid and Interface Science*, 1966, 22, 462-468.
2. K. J. Lissant and K. G. Mayhan, *Journal of Colloid and Interface Science*, 1973, 42, 201-208.
3. H. M. Princen, *Journal of Colloid and Interface Science*, 1979, 71, 55-66.
4. H. Kunieda, Y. Fukui, H. Uchiyama and C. Solans, *Langmuir*, 1996, 12, 2136-2140.
5. M. S. Silverstein, *Progress in Polymer Science*, 2014, 39, 199-234.
6. N. R. Cameron, *Polymer*, 2005, 46, 1439-1449.
7. P. Krajnc, N. Leber, J. F. Brown and N. R. Cameron, *Reactive and Functional Polymers*, 2006, 66, 81-91.
8. R. J. Wakeman, Z. G. Bhumgara and G. Akay, *Chemical Engineering Journal*, 1998, 70, 133-141.
9. I. Pulko, M. Kolar and P. Krajnc, *Science of The Total Environment*, 2007, 386, 114-123.
10. C. Zhao, E. Danish, N. R. Cameron and R. Katakly, *Journal of Materials Chemistry*, 2007, 17, 2446-2453.
11. G. Akay, M. A. Birch and M. A. Bokhari, *Biomaterials*, 2004, 25, 3991-4000.
12. H. Lim, A. Kassim, N. Huang, P. Khiewc and W. Chiu, *Colloids and Surfaces A: Physicochemical and Engineering Aspects*, 2009, 345, 211-218.
13. S. S. Manley, N. Graeber, Z. Grof, A. Menner, G. F. Hewitt, F. Stepanek and A. Bismarck, *Soft Matter*, 2009, 5, 4780-4787.
14. S. D. Kimmins and N. R. Cameron, *Advanced Functional Materials*, 2011, 21, 211-225.
15. A. Imhof and D. J. Pine, *Nature*, 1997, 389, 948-951.
16. R. Mezzenga, J. Ruokolainen, G. H. Fredrickson and E. J. Kramer, *Macromolecules*, 2003, 36, 4466-4471.
17. N. R. Cameron and D. C. Sherrington, *Macromolecules*, 1997, 30, 5860-5869.
18. K. Hariri, S. Al Akhrass, C. Delaite, P. Moireau and G. Riess, *Polymer International*, 2007, 56, 1200-1205.
19. D. Cai, J. H. T. Thijssen and P. S. Clegg, *ACS Applied Materials & Interfaces*, 2014, 6, 9214-9219.
20. N. Shirshova, A. Bismarck and J. H. G. Steinke, *Macromolecular Rapid Communications*, 2011, 32, 1899-1904.
21. J. Li, J. Zhang, Y. Zhao, B. Han and G. Yang, *Chemical Communications*, 2012, 48, 994-996.
22. N. Shirshova, P. Johansson, M. J. Marczewski, E. Kot, D. Ensling, A. Bismarck and J. H. G. Steinke, *Journal of Materials Chemistry A*, 2013, 1, 9612-9619.
23. E. Kot, N. Shirshova, A. Bismarck and J. H. G. Steinke, *RSC Advances*, 2014, 4, 11512-11519.
24. R. Butler, C. M. Davies and A. I. Cooper, *Advanced Materials*, 2001, 13, 1459-1463.
25. A. I. Cooper, *Advanced Materials*, 2003, 15, 1049-1059.
26. R. Butler, I. Hopkinson and A. I. Cooper, *Journal of the American Chemical Society*, 2003, 125, 14473-14481.
27. C. Boyere, A. Favrelle, A. F. Leonard, F. Boury, C. Jerome and A. Debuigne, *Journal of Materials Chemistry A*, 2013, 1, 8479-8487.
28. A. Carranza, J. A. Pojman and J. D. Mota-Morales, *RSC Advances*, 2014, 4, 41584-41587.
29. A. P. Abbott, D. Boothby, G. Capper, D. L. Davies and R. K. Rasheed, *Journal of the American Chemical Society*, 2004, 126, 9142-9147.
30. D. Carriazo, M. C. Serrano, M. C. Gutierrez, M. L. Ferrer and F. del Monte, *Chemical Society Reviews*, 2012, 41, 4996-5014.
31. E. L. Smith, A. P. Abbott and K. S. Ryder, *Chemical Reviews*, 2014, 114, 11060-11082.
32. F. del Monte, D. Carriazo, M. C. Serrano, M. C. Gutiérrez and M. L. Ferrer, *ChemSusChem*, 2014, 7, 999-1009.
33. A. Yadav and S. Pandey, *Journal of Chemical & Engineering Data*, 2014, 59, 2221-2229.
34. Q. Zhang, K. De Oliveira Vigier, S. Royer and F. Jerome, *Chemical Society Reviews*, 2012, 41, 7108-7146.
35. D. Barby, Z. Haq, Pat. 0.060.138, 1982 (to Unilever)
36. H. H. Chen and E. Ruckenstein, *Journal of Colloid and Interface Science*, 1991, 145, 260-269.

37. J. L. Anderson, V. Pino, E. C. Hagberg, V. V. Sheares and D. W. Armstrong, *Chemical Communications*, 2003, 2444-2445.
38. T. Inoue and T. Misono, *Journal of Colloid and Interface Science*, 2008, 326, 483-489.
39. H. Kunieda, N. Yano and C. Solans, *Colloids and Surfaces*, 1989, 36, 313-322.
40. J. M. Williams and D. A. Wroblewski, *Langmuir*, 1988, 4, 656-662.
41. J. M. Williams, A. J. Gray and M. H. Wilkerson, *Langmuir*, 1990, 6, 437-444.
42. I. Pulko and P. Krajnc, *Macromolecular Rapid Communications*, 2012, 33, 1731-1746.
43. N. R. Cameron, D. C. Sherrington, L. Albiston and D. P. Gregory, *Colloid Polym Sci*, 1996, 274, 592-595.
44. S. K. Maiti, L. J. Gibson and M. F. Ashby, *Acta Metallurgica*, 1984, 32, 1963-1975.
45. C. Solans and J. Esquena, *Emulsions and Emulsion Stability*, CRC Press, 2005.
46. S. Livshin and M. S. Silverstein, *Soft Matter*, 2008, 4, 1630-1638.
47. S. Vilchez, L. A. Pérez-Carrillo, J. Miras, C. Solans and J. Esquena, *Langmuir*, 2012, 28, 7614-7621.